New Journal of Physics
The open access journal at the forefront of physics

Deutsche Physikalische Gesellschaft **DPG**

IOP Institute of Physics

PAPER • OPEN ACCESS

Experimental generalized quantum suppression law in Sylvester interferometers

View the article online for updates and enhancements.

Related content

- Towards quantum supremacy with lossy scattershot boson sampling
  Ludovico Latmiral, Nicolò Spagnolo and Fabio Sciarrino

- Observation of photonic states dynamics in 3-D integrated Fourier circuits
  Fulvio Flamini, Niko Viggianiello, Taira Giordani et al.

- Interference of identical particles from entanglement to boson-sampling
  Malte C Tichy

Recent citations

- Observation of photonic states dynamics in 3-D integrated Fourier circuits
  Fulvio Flamini *et al*

New Journal of Physics

The open access journal at the forefront of physics

Deutsche Physikalische Gesellschaft ⏀ DPG

IOP Institute of Physics

Published in partnership with: Deutsche Physikalische Gesellschaft and the Institute of Physics

Experimental generalized quantum suppression law in Sylvester interferometers

Niko Viggianiello[1], Fulvio Flamini[1], Luca Innocenti[1,2] ⬤, Daniele Cozzolino[1,3], Marco Bentivegna[1], Nicolò Spagnolo[1], Andrea Crespi[4,5], Daniel J Brod[6,7], Ernesto F Galvão[7], Roberto Osellame[4,5] and Fabio Sciarrino[1]

1 Dipartimento di Fisica, Sapienza Università di Roma, Piazzale Aldo Moro 5, I-00185 Roma, Italy
2 Centre for Theoretical Atomic, Molecular and Optical Physics, School of Mathematics and Physics, Queen's University, Belfast BT7 1NN, United Kingdom
3 Dipartimento di Fisica, Università degli Studi di Napoli Federico II, Corso Umberto I, 40, I-80138 Napoli, Italy
4 Istituto di Fotonica e Nanotecnologie, Consiglio Nazionale delle Ricerche (IFN-CNR), Piazza Leonardo da Vinci, 32, I-20133 Milano, Italy
5 Dipartimento di Fisica, Politecnico di Milano, Piazza Leonardo da Vinci, 32, I-20133 Milano, Italy
6 Perimeter Institute for Theoretical Physics, 31 Caroline Street North, Waterloo, ON N2L 2Y5, Canada
7 Instituto de Física, Universidade Federal Fluminense, Av. Gal. Milton Tavares de Souza s/n, Niterói, RJ, 24210-340, Brazil

E-mail: fabio.sciarrino@uniroma1.it

Keywords: integrated interferometers, multi-photon interference, suppression law, generalized Hong–Ou–Mandel effect

Abstract

Photonic interference is a key quantum resource for optical quantum computation, and in particular for so-called boson sampling devices. In interferometers with certain symmetries, genuine multi-photon quantum interference effectively suppresses certain sets of events, as in the original Hong–Ou–Mandel effect. Recently, it was shown that some classical and semi-classical models could be ruled out by identifying such suppressions in Fourier interferometers. Here we propose a suppression law suitable for random-input experiments in multimode Sylvester interferometers, and verify it experimentally using 4- and 8-mode integrated interferometers. The observed suppression occurs for a much larger fraction of input–output combinations than what is observed in Fourier interferometers of the same size, and could be relevant to certification of boson sampling machines and other experiments relying on bosonic interference, such as quantum simulation and quantum metrology.

1. Introduction

Scalable, general-purpose quantum computers, once developed, will be able to solve problems believed to be intractable for ordinary computers. Given the significant technological challenges involved, other nearer-term goals for the field were suggested, such as the creation of quantum machines able to beat classical computers in particular computational tasks. One such proposal which has drawn much interest is boson sampling [1], which relies on multiphoton interference in a random linear interferometer, and whose output statistics are thought to be hard to sample classically. Due to bosonic interference, the output of those experiments is distributed according to the permanents of complex matrices specifying the interferometer's design, and the permanent is a function that is notoriously hard to calculate [1–3]. This possible path towards a demonstration of quantum computational supremacy has resulted in strong efforts to realize experimental implementations of such boson sampling devices [4–15].

To investigate the factors behind the computational complexity of these devices, different kinds of input states have been considered. It is known that inputs consisting of distinguishable photons, coherent states, and antisymmetric (fermionic-like) states all result in classically simulable behavior. On the other hand, photon-added coherent states [16] and quantum superpositions of coherent states (cat states) [17] have been claimed to yield hard-to-simulate outputs. Partially distinguishable photons seem to yield an intermediate regime deserving further investigation [18–21]. The effect of losses on simulation complexity was also considered

[22, 23]. Moreover, specific semi-classical states able to reproduce some collective interference effects while being efficiently simulable have been identified [24].

Other implementations of boson sampling devices serve to improve performance, or were used to discuss how to certify the correct functioning of the device. So-called scattershot boson sampling devices [12, 25, 26] use simultaneous pumping of several parametric down-conversion (PDC) sources to result in a random-input version of the original problem. The main advantage is a greatly enhanced generation rate, compared to a single-input implementations using the same sources. Other proposals suggest the adoption of squeezed states as a non-classical resource [27]. While complete certification of large boson sampling devices may turn out to be impossible, a number of proposals for partial certification were made, capable of comparing the experimental outcomes against some physically motivated error models [9, 10, 28–34].

As genuine many-particle interference is required for boson sampling, efforts have been directed at providing stronger evidence of this phenomenon. The simplest such demonstration is the Hong–Ou–Mandel (HOM) effect [35]. Generalizations of this effect have been proposed to investigate signatures of interference for specific input–output combinations of Fourier [11, 24, 36–38] and Sylvester [39] interferometers, and hypercube graphs [40]. These highly symmetric transformations provide a rich landscape for multi-particle interference to happen, which is the subject of our analysis.

In this work we discuss and experimentally demonstrate a zero-transmission law for Sylvester interferometers. As we will see, indistinguishable photons interfere in these devices so that a certain fraction of all input–output combinations are suppressed. This suggests they may be helpful in identifying multi-photon interference in random-input, scattershot boson sampling experiments. The zero-transmission law is demonstrated experimentally in Sylvester interferometers with $m = 4$ and $m = 8$ modes, implemented with the three-dimensional capabilities of femtosecond laser writing technology [41, 42].

2. Suppression law in Sylvester matrices

A suppression law, or equivalently zero-transmission law, is an efficient algorithm predicting that, for a given interferometer U, specific combinations of input/output states are strictly suppressed due to many-particle interference. Sylvester matrices are special constructions of Hadamard matrices of dimension $m = 2^p$, with p integer, whose elements are only $+1$ and -1 and can be defined as $H(2^p) = H^{\otimes p}$, where $H = \begin{pmatrix} 1 & 1 \\ 1 & -1 \end{pmatrix}$ is the unnormalized 2×2 Hadamard matrix. Sylvester matrices can be equivalently defined recursively as:

$$H(2^p) = \begin{pmatrix} H(2^{p-1}) & H(2^{p-1}) \\ H(2^{p-1}) & -H(2^{p-1}) \end{pmatrix}. \tag{1}$$

An analytic expression for the (i, j) element of a Sylvester matrix is given by $[H(2^p)]_{i,j} = (-1)^{i_B \odot j_B}$, where i_B and j_B are the binary representations of $i - 1$ and $j - 1$ respectively, and $\odot$ is the bitwise dot product, that is, the sum modulo 2 of the products of pairs of bits. The associated unitary transformation is a rescaled $U_S^m = m^{-1/2} H(m)$. When $p = 1$ we have the simplest Sylvester unitary, describing a symmetric 50:50 beam splitter. The celebrated HOM effect [35] is a first example of suppression law, as a transition between photons in input modes $(1, 2)$ and output modes $(1, 2)$ is strictly suppressed. A more general instance of this phenomenon was later identified by Tichy *et al* [24, 36], which proposed an efficient way to predict strict suppressions occurring in Fourier interferometers. This suppression law predicts that, for periodic inputs [43], a large number of output states corresponds to strictly vanishing scattering amplitudes. The number of input/output pairs that are predicted to be suppressed by this method is however very small with respect to the total number of states, because only a small class of input states satisfies the required symmetry properties of periodicity. This makes this protocol unsuitable in the context of scattershot boson sampling experiments, in which the input state changes randomly for every event. A different class of unitaries, the so-called Sylvester interferometers, was later considered in [39], and a new suppression law was derived for these matrices. The suppression law for Sylvester matrices identified in [39] considers n-photon input states, with $n = 2^q$, of the form $(1 + nc, \ldots, n + nc)$ with $0 \leqslant c \leqslant 2^k - 1$, injected in $2^{k+q} = m$-dimensional Sylvester interferometers. It was proven that all outputs whose bitwise sum of binary-represented mode occupation numbers is not the zero vector are strictly suppressed. This suppression law only identifies a small subset of all suppressed input–output combinations.

We now introduce a generalized law that identifies a larger number of suppressed input–output combinations in Sylvester interferometers. We are interested in the transition amplitudes between states of n photons in m modes, and restrict ourselves to the case $n \leqslant m$. An n-photon input configuration is described by the state vector $|r\rangle = |r_1 \ldots r_m\rangle$, where r_i is the number of photons occupying mode i. A general n-photon input configuration may be represented also by a mode assignment list (MAL) $\tilde{r} = (\tilde{r}_1, \tilde{r}_2, \ldots, \tilde{r}_n)$, where $\tilde{r}_j$ specifies which modes are occupied. As an example, an input state with $n = 4$ and $m = 8$ with one photon in each of the first four modes is described by the state vector $|r\rangle = |1, 1, 1, 1, 0, 0, 0, 0\rangle$ and by the MAL $\tilde{r} = (1, 2, 3, 4)$.

Since photons are indistinguishable, the ordering of elements in the MAL is meaningless, and we conventionally choose the list to be in nondecreasing order. It will be useful to represent this state as a $n \times p$ binary matrix (BM) R, whose ith row is the binary representation of $\tilde{r}_i - 1$ (padded with zeros on the left so it has length p). Similarly to MALs, the order of the rows of such BM representation is irrelevant, i.e. if R and R' are related only by a permutation of the rows, they represent the same physical state. We will denote this equivalence relation between binary matrices as $R \sim R'$. Let us call $\mathcal{N}^A(R)$ the matrix obtained by negating each bit in the columns of R specified by a list of indices A. As an example, for $m = 8$ and $n = 4$ consider state $|r\rangle = |1, 1, 1, 1, 0, 0, 0, 0\rangle$, corresponding to the MAL $\tilde{r} = (1, 2, 3, 4)$. Then we have

$$R = \begin{pmatrix} 0 & 0 & 0 \\ 0 & 0 & 1 \\ 0 & 1 & 0 \\ 0 & 1 & 1 \end{pmatrix} \quad \mathcal{N}_R^{\{1,3\}} = \begin{pmatrix} 1 & 0 & 1 \\ 1 & 0 & 0 \\ 1 & 1 & 1 \\ 1 & 1 & 0 \end{pmatrix} \quad \mathcal{N}_R^{\{1,2,3\}} = \begin{pmatrix} 1 & 1 & 1 \\ 1 & 1 & 0 \\ 1 & 0 & 1 \\ 1 & 0 & 0 \end{pmatrix}. \tag{2}$$

Similarly, $\mathcal{N}^{\{2\}}(R) \sim \mathcal{N}^{\{3\}}(R) \sim R$, since they are related to each other by permutations of their rows, whereas $\mathcal{N}^{\{1\}}(R)$ represents a different state.

The input–output combinations $|r\rangle \rightarrow |s\rangle$ and $|s\rangle \rightarrow |r\rangle$ are suppressed if some A exists for which the following two conditions are met.

Condition I. For a given input $|r\rangle$ with BM representation R, check whether R has any subsets of columns A such that negating those columns of R results in R up to a permutation of the rows:

$$\mathcal{N}^A(\tilde{r}) = \tilde{r}. \tag{3}$$

Condition II. Consider any output $|s\rangle$ with BM representation S and any $A \in \mathcal{A}$. If the columns A of S contain an odd number of 1s, the transition from R to S is suppressed:

$$\bigoplus_{k=1}^{n} \bigoplus_{\alpha \in A} S_{k,\alpha} = 1. \tag{4}$$

Here, $\bigoplus$ denotes the bitwise sum, that is, a sum modulo 2 performed separately for each bit. The conditions of the generalized suppression law are never satisfied when n is odd. As an example, let us again consider state $|r\rangle = |1, 1, 1, 1, 0, 0, 0, 0\rangle$. We have $\mathcal{N}^A(\tilde{r}) = \tilde{r}$ for $A = \{2\}, A = \{3\}$. and $A = \{2, 3\}$. Equations (3), (4) predicts suppression of all output states whose binary representation has an odd number of 1s in either the second column, the third column, or in the second and third columns combined. For example, the states $\tilde{s}_1 = (3, 6, 7, 8)$, $\tilde{s}_2 = (2, 6, 7, 8)$, and $\tilde{s}_3 = (4, 6, 7, 8)$, having binary representations

$$R_1 = \begin{pmatrix} 0 & 1 & 0 \\ 1 & 0 & 1 \\ 1 & 1 & 0 \\ 1 & 1 & 1 \end{pmatrix} \quad R_2 = \begin{pmatrix} 0 & 0 & 1 \\ 1 & 0 & 1 \\ 1 & 1 & 0 \\ 1 & 1 & 1 \end{pmatrix} \quad R_3 = \begin{pmatrix} 0 & 1 & 1 \\ 1 & 0 & 1 \\ 1 & 1 & 0 \\ 1 & 1 & 1 \end{pmatrix} \tag{5}$$

respectively, are all suppressed. In appendix A we give a proof of this law, while a calculation of the asymptotic behavior for the fraction of suppressed events these criteria identify can be found in appendix B. While this work was under completion, a similar suppression criterion was proposed in [40] for hypercube graphs. In appendix A we show that the interferometers and criteria of [40] are actually equivalent to ours. In the $n = 2$ case, and therefore for the experimental implementations reported below, our criterion identifies all suppressed events, which are more numerous than the equivalent result for Fourier matrices [24] with the same size. In figure 1 we see how 8-mode Sylvester and Fourier matrices compare in terms of suppressed transitions for 2 and 4 photons, where it is clear that the Sylvester matrix outperforms the Fourier one.

For small values of n and m it is also possible to exactly compute the fraction of suppressed input–output pairs (including those not detected by the discussed suppression law), which we report in table 1. This table shows that the Sylvester matrix does indeed perform better than the Fourier matrix for most cases, although there are cases in which no suppression is given by Sylvester interferometers. For instance, in table 1 we observe that, within the investigated regime, the fraction of suppressed configurations is 0 when the number of photons is $2^p - 1$ for all p. Moreover the presented suppression law applies when the number of photons is even, as opposed to the suppression law for Fourier interferometers which works for all values of n, and the one presented in [39] which works for only $n = 2^q$. For $n = 3$ and 7, for example, it is possible to show that there can be no suppressed transitions for Sylvester matrices (this is a consequence of the fact that the permanent of a $(2^p - 1) \times (2^p - 1)$ matrix where all elements are ± 1, for integer p, is never zero [44]), whereas the Fourier matrix does contain a few suppressions. Note also that, for all cases reported in table 1 where the test of conditions I and II can be applied, the total number of suppressed pairs for Fourier matrices is not only smaller than the corresponding quantity for Sylvester matrices, but smaller even than the subset of input–output pairs that our test detects.
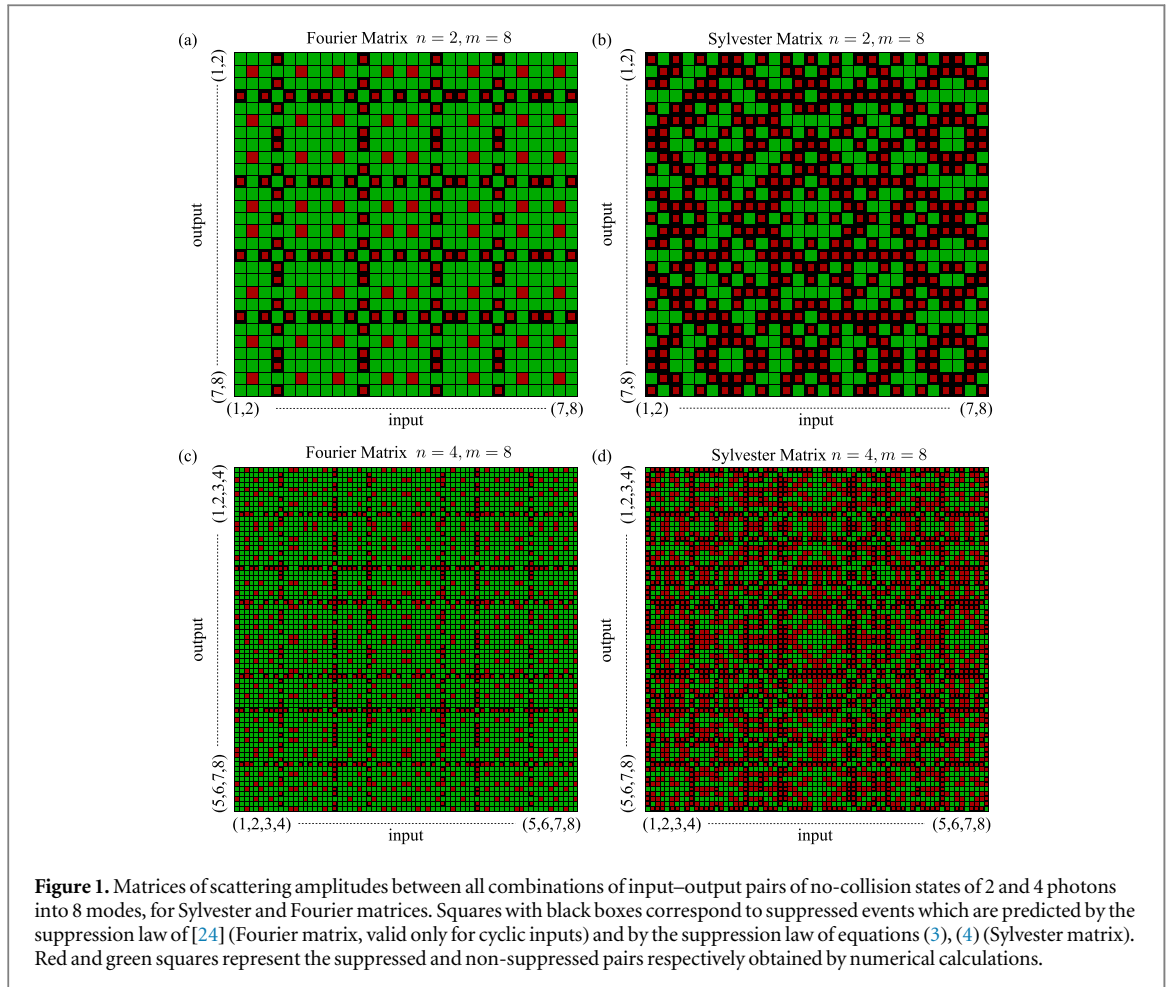
Figure 1. Matrices of scattering amplitudes between all combinations of input–output pairs of no-collision states of 2 and 4 photons into 8 modes, for Sylvester and Fourier matrices. Squares with black boxes correspond to suppressed events which are predicted by the suppression law of [24] (Fourier matrix, valid only for cyclic inputs) and by the suppression law of equations (3), (4) (Sylvester matrix). Red and green squares represent the suppressed and non-suppressed pairs respectively obtained by numerical calculations.

Table 1. Fractions of suppressed pairs for Sylvester and Fourier matrices, for several values of *m* modes and *n* photons. The column Sylvester (All) reports all suppressed pairs, and the column Sylvester (Test) only those detected by the discussed suppression law. Note that the test described in such law only works for even values of *n*. Numbers indicated by an * are estimates obtained by sampling 500000 different input–output pairs, all others are exact.

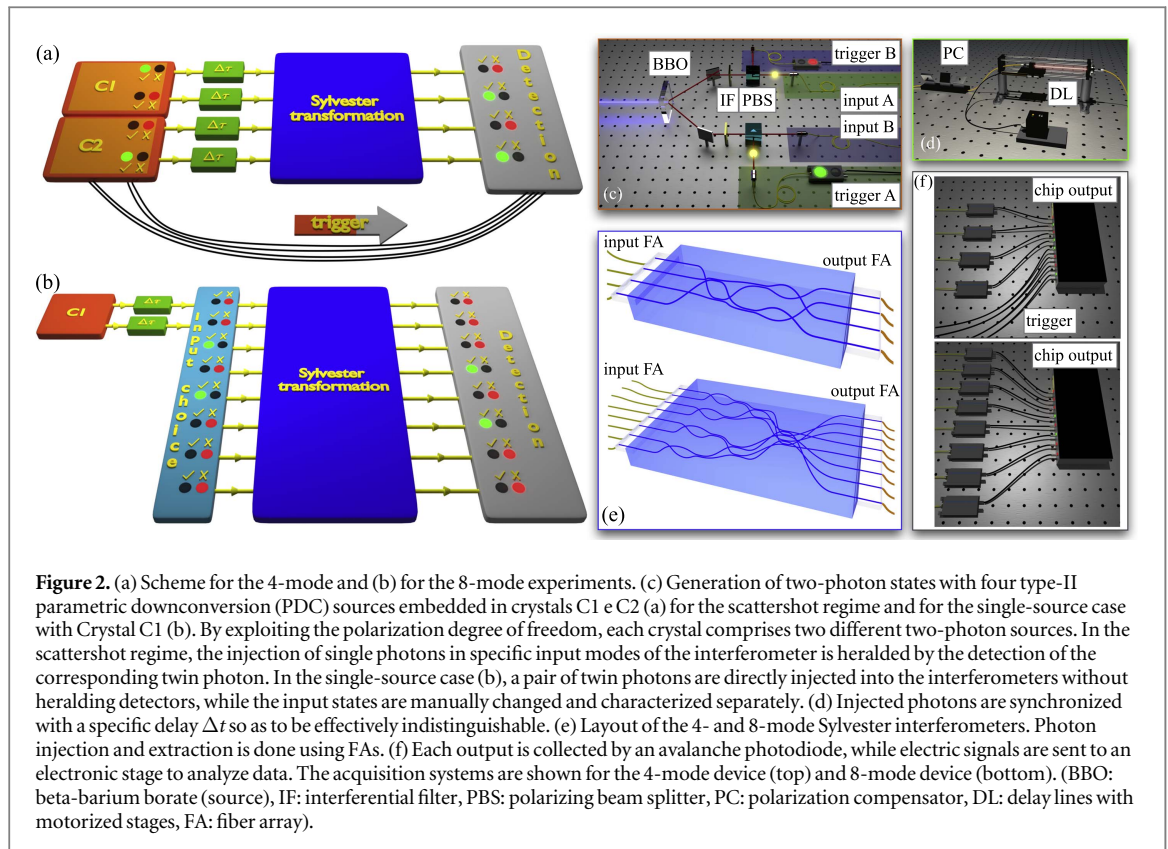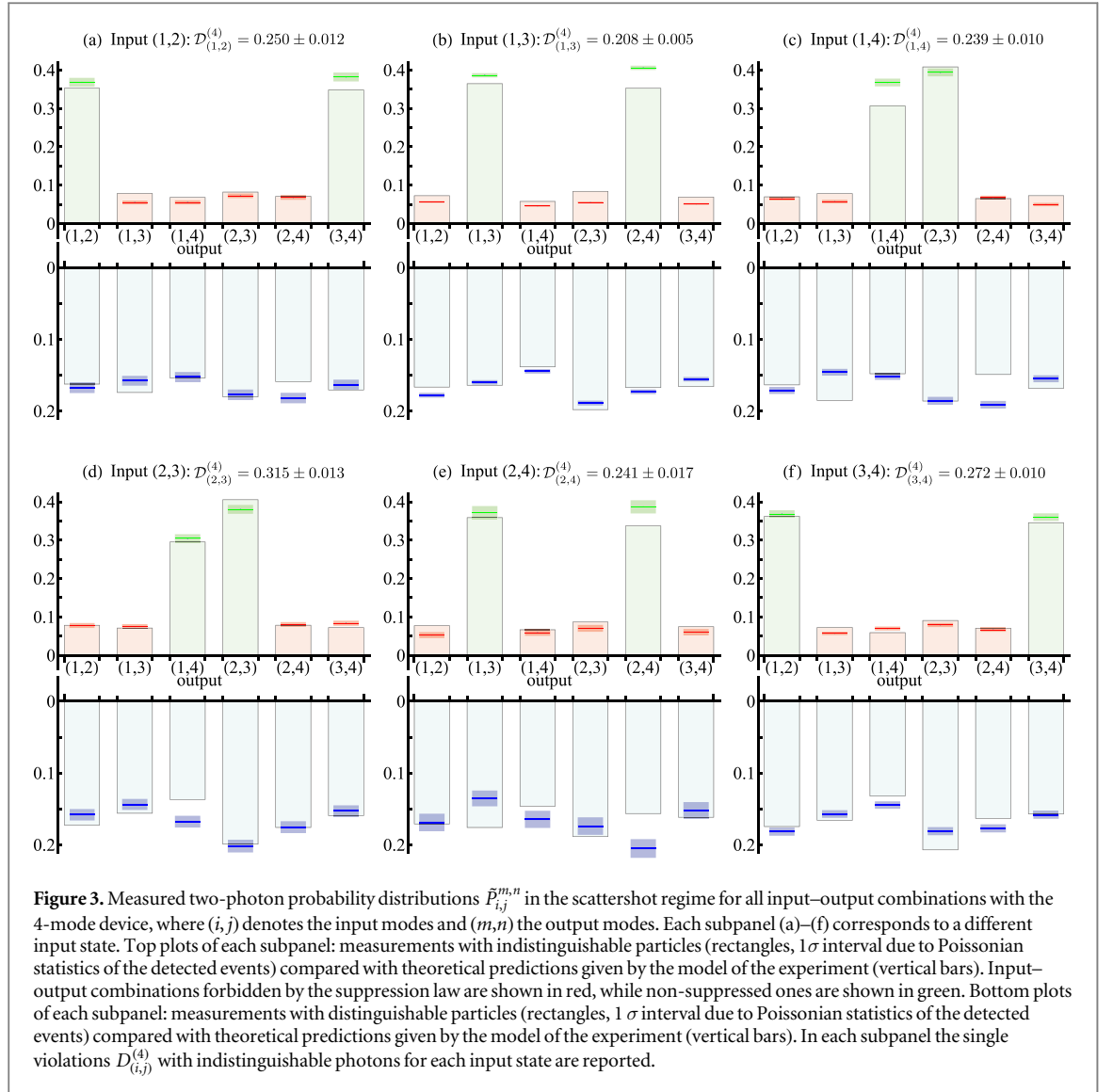| m	n	Sylvester (All)	Sylvester (Test)	Fourier
4	2	66.7%	66.7%	44.4%
	3	0	0	0
8	2	57.14%	57.14%	24.49%
	3	0	0	16.33%
	4	54.86%	27.42%	21.22%
	5	57.14%	0	24.49%
	6	57.14%	57.14%	48.98%
	7	0	0	0
16	2	53.33%	53.33%	14.22%
	3	0	0	5.22%
	4	40.57%	11.5%	5.37%
	5	40.57%	0	2.54%
	6	37.14%	9.9%*	2.32%
	7	0	0	0.88%*
	8	26.24%	6.9%*	1.20%

Figure 2. (a) Scheme for the 4-mode and (b) for the 8-mode experiments. (c) Generation of two-photon states with four type-II parametric downconversion (PDC) sources embedded in crystals C1 e C2 (a) for the scattershot regime and for the single-source case with Crystal C1 (b). By exploiting the polarization degree of freedom, each crystal comprises two different two-photon sources. In the scattershot regime, the injection of single photons in specific input modes of the interferometer is heralded by the detection of the corresponding twin photon. In the single-source case (b), a pair of twin photons are directly injected into the interferometers without heralding detectors, while the input states are manually changed and characterized separately. (d) Injected photons are synchronized with a specific delay Δt so as to be effectively indistinguishable. (e) Layout of the 4- and 8-mode Sylvester interferometers. Photon injection and extraction is done using FAs. (f) Each output is collected by an avalanche photodiode, while electric signals are sent to an electronic stage to analyze data. The acquisition systems are shown for the 4-mode device (top) and 8-mode device (bottom). (BBO: beta-barium borate (source), IF: interferential filter, PBS: polarizing beam splitter, PC: polarization compensator, DL: delay lines with motorized stages, FA: fiber array).

3. Experimental generalized suppression law

The generalized suppression law has been tested experimentally in 4- and 8-mode Sylvester interferometers, implemented by exploiting a 3D architecture enabled by femtosecond laser writing [37] (see figure 2). We performed a two-photon scattershot boson sampling experiment [12] to verify the suppression law, feeding each input port of the 4-mode chip with one heralded photon from a different PDC pair. The output events corresponding to two-photon injection were then post-selected via four-fold coincidence measurements (two heralding detectors and two detectors at the output of the device) for all the $\binom{4}{2} = 6$ input–output combinations. In such a way, the apparatus is able to sample all no-collision input–output states, i.e., those configurations where no more than one photon is present for each input and output port. The experimental setup adopted for the scattershot approach is shown in figure 2. Further details on the generation and detection are reported in appendix C.

The observed two-photon output statistics are shown in figure 3, where one can recognize the pattern of peaks and dips predicted by the Sylvester matrix (U_S^4). As a first step, in figure 3 we report the comparison between the experimental data and the theoretical predictions obtained by a model taking into account the main sources of errors (discussed in details in appendix D). In this scattershot experiment, three main imperfections affect the measured data: (i) fabrication errors in the unitary transformation, (ii) multi-photon emission from the source, and (iii) partial indistinguishability of the heralded photons. Effect (i) leads to a non-unitary fidelity between the implemented transformation and the Sylvester one. This can be checked by performing a tomography of the unitary transformation. The tomography has been achieved by measuring all single-photon probabilities and two-photon HOM visibilities, and by minimizing a χ^2 function to retrieve the physical parameters of the device (directional coupler transmittivities and internal phases) that best reproduce the observed experimental data [37, 45]. A figure of merit to quantify the adherence of the implemented transformation with the Sylvester one is the fidelity *F*, defined between two unitary matrices *U* and *V* as $F = 1/m |\operatorname{Tr}(UV^{\dagger})|$ where *m* is the matrix dimension. In our experiment, such fidelity attains a value close to unity $\mathcal{F} = 0.99807 \pm 0.00005$, and thus error (i) is small and negligible with respect to (ii)–(iii). Error source (ii) is due to the probabilistic nature of PDC, which leads to a non-zero probability of emission of two photon pairs from a single source. In presence of non photon-number resolving detectors and losses, multi-photon emission leads to noise contributions that cannot be discriminated from the correct evolution. In our experiment, effect (ii) is approximately ~3% of all collected events. Partial indistinguishability of the heralded photons (iii) is due to the presence of spectral correlations between photons belonging to the same pair. This can be modeled by an

Figure 3. Measured two-photon probability distributions $\tilde{P}_{i,j}^{m,n}$ in the scattershot regime for all input–output combinations with the 4-mode device, where (i, j) denotes the input modes and (m,n) the output modes. Each subpanel (a)–(f) corresponds to a different input state. Top plots of each subpanel: measurements with indistinguishable particles (rectangles, 1σ interval due to Poissonian statistics of the detected events) compared with theoretical predictions given by the model of the experiment (vertical bars). Input–output combinations forbidden by the suppression law are shown in red, while non-suppressed ones are shown in green. Bottom plots of each subpanel: measurements with distinguishable particles (rectangles, 1σ interval due to Poissonian statistics of the detected events) compared with theoretical predictions given by the model of the experiment (vertical bars). In each subpanel the single violations $D_{(i,j)}^{(4)}$ with indistinguishable photons for each input state are reported.

indistinguishability parameter, which in our experiment reaches the value $p = 0.758 \pm 0.008$ (see appendix D). A good agreement between the experimental data with indistinguishable photons and the model is found, and is confirmed by the variation distance $d = 1/2\sum_\alpha |P_\alpha^{\mathrm{exp}} - P_\alpha^{\mathrm{mod}}|$ between data P_α^{exp} and the predictions P_α^{mod}. For the reported experiment, the value d averaged over the input states is $\bar{d} = 0.053 \pm 0.021$. Analogously, the same analysis is performed for experimental data collected with distinguishable photons. Again the good agreement is confirmed by the distance $\bar{d} = 0.045 \pm 0.016$, averaged over the input states, between the model and the measured data.

An effective figure of merit to estimate if the observed data are compatible with those expected from a fully interfering multiphoton source is the degree of violation $\mathcal{D} = N_{\mathrm{forbidden}}/N_{\mathrm{events}}$ [24, 37]. Here, $N_{\mathrm{forbidden}}$ is the number of events which occur in an input–output combination which is predicted to be suppressed by equations (3), (4), while N_{events} is the total number of measured events. In an ideal scenario with indistinguishable photons evolving in a Sylvester transformation, the degree of violation is equal to zero. Evaluating the observed violation permits to rule out alternative hypotheses on the nature of the injected state. More specifically, if the observed value of $\mathcal{D}$ is significantly smaller than the expected value for a given model, that hypothesis can be excluded as a possible explanation of the data. The simplest case is that the n photons are distinguishable. A more elaborate alternative model is the mean field (MF) state [24, 46, 47], defined as a single-particle state whose wavefunction is macroscopically spread over a set of inputs A: $|\psi_{\mathrm{MF}}^A\rangle = n^{-1/2}\sum_{r \in A}e^{i\theta_r}|j_r\rangle$, where $|j_r\rangle$ identifies a single-photon state in mode j_r, and phases θ_r are randomly chosen from a uniform distribution. Summing the output statistics of n states of this form reproduces some macroscopic interference effects [10] of n indistinguishable photons injected in modes A. Note that suppression laws are only partially fulfilled by MF states statistics, which confirms the diagnostic power of these tools. In particular, it is easy to check that the expected degree of violation for distinguishable particles and MF states in U_S^4 are respectively 0.66
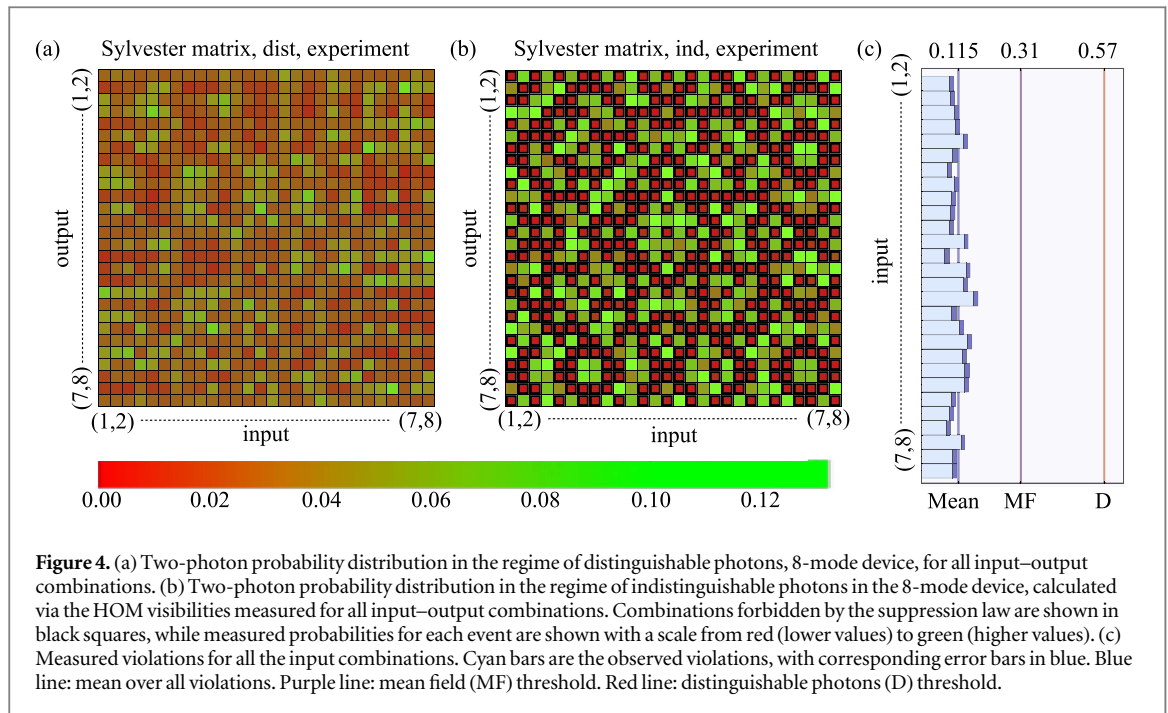
Figure 4. (a) Two-photon probability distribution in the regime of distinguishable photons, 8-mode device, for all input–output combinations. (b) Two-photon probability distribution in the regime of indistinguishable photons in the 8-mode device, calculated via the HOM visibilities measured for all input–output combinations. Combinations forbidden by the suppression law are shown in black squares, while measured probabilities for each event are shown with a scale from red (lower values) to green (higher values). (c) Measured violations for all the input combinations. Cyan bars are the observed violations, with corresponding error bars in blue. Blue line: mean over all violations. Purple line: mean field (MF) threshold. Red line: distinguishable photons (D) threshold.

and 0.4 (considering only collision-free two-photon inputs and outputs). The overall experimental violation $\mathcal{D}$, obtained by summing all the measured events over all possible input–output combinations, is found to be $\mathcal{D}^{(4)} = 0.238 \pm 0.003$. The measured value, below the two thresholds by respectively 141 (distinguishable) and 54 (MF) standard deviations, thus unambiguously excludes both these hypotheses (figure 3).

The suppression law has been experimentally verified also using a Sylvester 8-mode chip, where the full set of $\binom{8}{2} = 28$ two-photon no-collision input states were independently investigated. In figure 4 we report the full set of 28×28 experimental probabilities, retrieved from the HOM visibilities measured for all no-collision input–output combinations. In this case, one can show that the theoretical degrees of violation for distinguishable particles and MF states are respectively 0.57 and 0.31. The mean value of the violations is $\bar{\mathcal{D}}^{(8)} = 0.115 \pm 0.002$, well below the theoretical bounds predicted for MF and distinguishable particles, thus ruling out these alternative hypotheses.

4. Conclusions and discussion

We introduced and verified experimentally a suppression law pertinent to Sylvester interferometers with indistinguishable photons as inputs. The choice of this unitary transformation ensures a significant fraction of suppressed input–output combinations, even for a larger number of photons and modes. For example, for $n = 6$ and $m = 16$ our law predicts the suppression of ~10% of the input–output combinations, compared to a total fraction of forbidden events of ~37% (computed numerically), against just ~2.3% for the Fourier matrix [24, 37]. This suppression can be useful towards identification of genuine multiphoton interference also in scattershot boson sampling experiments, where the full set of possible input states is employed. Indeed, random-input generation has been recognized as a promising approach to greatly enhance the event rate in PDC-based scattershot boson sampling experiments [12]. In this case, while the fraction of predicted suppressions vanishes exponentially, we find that there is a significant fraction of forbidden configurations which are not detected by the proposed law, thus encouraging further investigation for a theorem that holds in the more general case. We have shown that the suppression law is able to rule out alternative models that display coarse-grained interference effects. Its application will be helpful in testing boson sampling experiments, in cooperation with techniques suitable to study the overall transformations [31], as well as in assessing the degree of indistinguishability of single-photon sources, thanks to the high-sensitivity of Sylvester interferometers to multi-photon interference.

Acknowledgments

Appendix A. Suppression law for Sylvester matrices

In this appendix we present a proof of the test that generalizes the one of [39], predicting a higher fraction of suppressed pairs. This test can be assessed with a computational cost increasing only polynomially in *m* and *n*. After proving the test is sound, we will show it is equivalent to a test proposed independently in [40], using a different formalism. Let us begin with the following two straightforward lemmas.

Lemma 1. *Let S_n be the set of permutations of $\{1, \ldots, n\}$, and let $\tau \in S_n$ be a permutation different from the identity such that $\tau^2 = \mathbb{1}$. Then we can uniquely associate to each $\sigma \in S_n$ another (different) permutation $\sigma_\tau \equiv \tau \circ \sigma$, where $\circ$ denotes the composition of permutations.*

This lemma directly follows from the observation that S_n is a finite group. For the suppression law described in this article, it is however useful to remark this way to associate to each permutation another permutation. In fact, the core principle behind the suppression law will be that, provided some conditions are satisfied, one can find a τ such that, for every σ, the contributions to the amplitude given by σ and σ_τ cancel each other out.

Lemma 2. *Let $\tilde{r}$, R and $\mathcal{N}^A$ be as in section 2. Then $\mathcal{N}^A(\tilde{r}) = \tilde{r}$ if and only if $\mathcal{N}^A(R) \sim R$. This, in turn, happens if and only if there is a permutation $\tau \in S_n$ such that $\mathcal{N}^A(R) = R^\tau$, where R^τ is obtained from R by applying the permutation τ to the rows of R. Now, if τ is such a permutation, we have*

  (i) $\tau \neq \mathbb{1}$,

 (ii) $\tau^2 = \mathbb{1}$,

(iii) *for each $\sigma \in S_n$, $\mathcal{N}^A(R^\sigma) = R^{\tau \circ \sigma}$*

(iv) *all columns of R in A have an equal number of 1s and 0s,*

 (v) *all columns of R not in A have an even number of 1s and an even number of 0s.*

Proof.

 (i) By definition, $\mathcal{N}^A(R)$ flips all elements of columns of R corresponding to the set A. If τ is the trivial permutation, $\mathcal{N}^A(R) = R$, which is not possible unless A empty.

 (ii) $\mathcal{N}^A$ applied twice to a BM clearly acts as the identity, from which follows immediately that $\tau^2 = \mathbb{1}$.

(iii) This can be seen from the explicit expression of $\mathcal{N}^A(R)$:

$$\mathcal{N}^A(R) \equiv \begin{cases} 1 \oplus R_{k,\alpha}, \ \alpha \in A, \\ R_{k,\alpha}, \ \alpha \notin A. \end{cases} \tag{A.1}$$

(iv) Take some column of R in A. By assumption, there is an operation composed of flipping every element followed by some permutation that leaves it invariant. Flipping every element switches the number of ones and zeroes, whereas a permutation preserves them, and so the number of ones and zeroes must be the same. Clearly this holds for all columns of R in A.

 (v) If $\mathcal{N}^A(R) = R^\tau$, the action of τ on the columns of R in A implies it is a permutation that maps half of the rows of R onto the other half. But τ must also act as the identity on the rows of R that are not in A, and so each of these halves must contain the same number of ones and zeroes, which means there is an even number of both in R.

□

We are now ready to state the main result for our suppression law:

Theorem 1. *Let $|r\rangle$ and $|s\rangle$ be two states of n particles in $m = 2^p$ modes, with corresponding mode occupation lists $\tilde{r}$ and $\tilde{s}$, and BM representations R and S. If there is a subset A of the columns of R such that*

$$\begin{cases} \mathcal{N}^A(\tilde{r}) = \tilde{r} \\ \displaystyle\bigoplus_{k=1}^{n} \bigoplus_{\alpha \in A} S_{k,\alpha} = 1 \end{cases}\text{,} \tag{A.2}$$

then the transition from $|r\rangle$ to $|s\rangle$ (and consequently also that from $|s\rangle$ to $|r\rangle$), when transversing the Sylvester interferometer, is suppressed.

Proof. The transition amplitude from $|r\rangle$ to $|s\rangle$ can be written as

$$\mathcal{A} := \frac{1}{\sqrt{r_1! \dots r_m! s_1! \dots s_m!}} \text{Per}(U_{r,s}), \tag{A.3}$$

where $\text{Per}(U)$ denotes the permanent of U. In the equation above, $U_{r,s}$ is the matrix defined element-wise as

$$[U_{r,s}]_{i,j} := \frac{1}{\sqrt{m}} [H(2^p)]_{\tilde{r}_i, \tilde{s}_j}, \tag{A.4}$$

where we recall $H(2^p)$ is the Sylvester matrix (see definition 1). Using the closed form expression for the elements of a Sylvester matrix, with equations (A.3) and (A.4), and denoting with $\mathbf{M}_i$ the ith row of matrix M, we obtain

$$\mathcal{A} = D \sum_{\sigma \in S_n} \prod_{k=1}^{n} (-1)^{\mathbf{R}_{\sigma(k)} \odot \mathbf{S}_k} = D \sum_{\sigma \in S_n} (-1)^{\mathcal{E}(\sigma)}, \tag{A.5}$$

where $\mathbf{B} \odot \mathbf{C}$ denotes the *bitwise dot product* between vectors $\mathbf{B}$ and $\mathbf{C}$, defined as $\mathbf{B} \odot \mathbf{C} := \bigoplus_{\alpha=1}^{p} B_\alpha C_\alpha$, D is a constant factor, and we defined

$$\mathcal{E}(\sigma) \equiv \bigoplus_{k=1}^{n} \mathbf{R}_{\sigma(k)} \odot \mathbf{S}_k = \bigoplus_{k=1}^{n} \bigoplus_{\alpha=1}^{p} R_{\sigma(k),\alpha} S_{k,\alpha}. \tag{A.6}$$

Since we are interested in whether $\mathcal{A} = 0$, we will ignore the constant factor D in (A.5). Clearly, for $\mathcal{A}$ to vanish, we need exactly half of the permutations to be such that $(-1)^{\mathcal{E}(\sigma)} = 1$. A necessary and sufficient condition for this to hold is if, for each permutation σ, we can uniquely assign another permutation σ' such that $\mathcal{E}(\sigma') = 1 \oplus \mathcal{E}(\sigma)$. From lemmas 1 and 2, we know that if condition (A.2) holds we can uniquely associate to each σ another permutation $\sigma_\tau \equiv \tau \circ \sigma$, where τ is the permutation such that $\mathcal{N}^A(R) = R^\tau$. Using σ_τ in (A.6) we have

$$\begin{aligned} \mathcal{E}(\sigma_\tau) &= \bigoplus_{k=1}^{n} \bigoplus_{\alpha=1}^{p} R_{\tau(\sigma(k)),\alpha} S_{k,\alpha} \\ &= \bigoplus_{k=1}^{n} \left[\left(\bigoplus_{\alpha \in A} R_{\tau(\sigma(k)),\alpha} S_{k,\alpha} \right) \oplus \left(\bigoplus_{\alpha \notin A} R_{\tau(\sigma(k)),\alpha} S_{k,\alpha} \right) \right]. \end{aligned} \tag{A.7}$$

Using now the explicit expression for $\mathcal{N}^A(R)$ and lemma 2, we have

$$\mathcal{N}^A(R^\sigma) = R^{\tau \circ \sigma} \iff \begin{cases} 1 \oplus R_{\sigma(k),\alpha} = R_{\tau(\sigma(k)),\alpha} & \text{for } \alpha \in A \\ R_{\sigma(k),\alpha} = R_{\tau(\sigma(k)),\alpha} & \text{for } \alpha \notin A \end{cases}. \tag{A.8}$$

Using the above in (A.7), and by using (A.2), we finally obtain

$$\mathcal{E}(\sigma_\tau) = \mathcal{E}(\sigma) \oplus \left[\bigoplus_{k=1}^{n} \bigoplus_{\alpha \in A} S_{k,\alpha} \right] = \mathcal{E}(\sigma) \oplus 1. \tag{A.9}$$

Using this last result in (A.5) we conclude that

$$\mathcal{A} = C \sum_{\sigma \in S_n} (-1)^{\mathcal{E}_{R,S}(\sigma)} \propto \sum_{\sigma \in S_n : \mathcal{E}(\sigma) \text{ even}} [(-1)^{\mathcal{E}(\sigma)} + (-1)^{\mathcal{E}(\sigma_\tau)}] = 0 \tag{A.10}$$

which proves that the input–output pair $(|r\rangle, |s\rangle)$ is suppressed. $\qquad\square$

Remark. (Efficiency) To check if theorem 1 applies to a given input–output pair, one has to verify condition (A.2) for each one of the $2^p - 1 = m - 1$ possible (non-empty) subsets of the p columns of R and S, which requires only a polynomial (in n and m) number of elementary operations. Hence, the proposed suppression law is efficiently verifiable.

While (A.2) gives a sufficient condition for an input–output pair to be suppressed, it is not necessary. For most input states, not all suppressed outputs satisfy theorem 1. In appendix B we give estimates of the fraction of states our test identifies as suppressed.

We now show that our suppression criterion for Sylvester matrices corresponds exactly to that obtained in [40] for hypercube graphs. These criteria were obtained independently, and use different formalisms. In [40], the unitary describing the dynamics of n bosons in a hypercube graph is given by

$$U = \frac{1}{\sqrt{2^p}} \begin{pmatrix} 1 & i \\ i & 1 \end{pmatrix}^{\otimes p}. \tag{A.11}$$

This is the same unitary evolution implemented by a Sylvester interferometer with 2^p modes, except for unimportant local phase shifts. As in our case, the criterion of [40] identifies symmetries that the n-photon input must satisfy. It is convenient to describe the input as a p-bit string $\vec{r}$, with ones indicating where single input photons are present, and zeros where no photon is present. The symmetries considered in [40] correspond to the $(2^p - 1)$ different products of the p different permutations described by a tensor product of a single X matrix and $(p - 1)$ 2×2 identity matrices:

$$S_i = \mathbb{1} \otimes \mathbb{1} \otimes \ldots \otimes X_i \otimes \mathbb{1} \otimes \ldots \mathbb{1}, \tag{A.12}$$

with i ranging from 1 to p. Each symmetry S divides the set of 2^p strings into two subsets of equal size, corresponding to the eigenspaces of S with eigenvalues ± 1. Our criterion considers subsets A of indices that determine which columns of the BM representation R of the input state will be negated. There are exactly $2^p - 1$ possible such subsets of indices, and negating bits of R in accordance to a given subset A corresponds to implementing exactly one of the permutations above. Both criteria require that the input state $\vec{r}$ be invariant under at least one such permutation.

If the input (represented by $\vec{r}$) is invariant under some of these symmetries, we must then test whether the condition over the output $\vec{s}$ is satisfied. In [40], for suppression it is required that an odd number of photons be in each ± 1 eigenspace of the identified input symmetry. This is exactly equivalent to our condition on the outputs. This shows that our suppression criteria is exactly equivalent to the criteria proposed by [40].

Appendix B. Estimates on fraction of suppressed states

In this appendix, we give estimates on the fraction of suppressed input–output pairs identified by the conditions of theorem 1, particularly focusing on upper bounds and asymptotic limits (in the number of modes m and photons n). Throughout this appendix, we are still restricted to $m = 2^p$ for some integer p, which means all binary matrices are $n \times p$, and to $n \leqslant m$. The fractions we obtain consider mainly the set of all possible states, $G_{n,m}$, which has $|G_{n,m}| = \binom{m + n - 1}{n}$ elements. At the end of this appendix we discuss the applicability of our results to the restriction of no-collision states.

We begin by restating the two conditions of theorem 1 informally, as they would be used in a test. For simplicity, we refer to the states $|r\rangle$ and $|s\rangle$ of theorem 1 as input and output states, respectively, although any conclusions can be extended to the case where the roles of input and output are reversed. With this in mind, we note that condition of equation (3) concerns only inputs, and we restate it as:

Condition I. For a given input with BM representation R, check whether R has any subsets of columns A such that negating those columns of R results in R up to a permutation of the rows (i.e. $\mathcal{N}^A(R) \sim R$).

Let us call $\mathcal{A}$ the set of all such subsets of columns A. For the state in example 2, for instance, $\mathcal{A} = \{\{2\}, \{3\}, \{2, 3\}\}$. If condition I finds no such A, the test fails to identify any suppressed transitions. Also, as a consequence of lemma 2, the test only works if n is even. Assuming that condition I yielded some non-empty $\mathcal{A}$, we can test for condition of equation (4), which is a test only on the outputs and which we restate as:

Condition II. Consider any output with BM representation S and any $A \in \mathcal{A}$. If the columns A of S contain an odd number of 1s, the transition from R to S is suppressed.

For simplicity, we begin by estimating how many output states are suppressed given that condition I identified a non-empty set $\mathcal{A}$ for some input. Before that, we need one final definition. We say that the elements of $\mathcal{A}$ are independent if none can be replaced by a sequence of the others. That is, if there is no $A \in \mathcal{A}$ and $A_1, A_2, \ldots, A_k \in \mathcal{A} \setminus \{A\}$ such that $\mathcal{N}^{A_1}(\mathcal{N}^{A_2} \ldots (\mathcal{N}^{A_k}(X))) = \mathcal{N}^A(X)$ for all binary matrices X. To illustrate this, consider example 2. There, $\mathcal{A} = \{\{2\}, \{3\}, \{2, 3\}\}$. Clearly, negating columns $\{2, 3\}$ of a BM is the same as negating column $\{2\}$ followed by column $\{3\}$. Furthermore, condition II can only be satisfied for $\{2, 3\}$ if it is satisfied by either $\{2\}$ or $\{3\}$. Thus, including $\{2, 3\}$ in $\mathcal{A}$ does not give any new suppressions beyond those identified by $\{2\}$ and $\{3\}$, so we can safely drop it (we could have dropped either $\{2\}$ or $\{3\}$ instead, to the same effect). Since the binary matrices have p columns, there can be at most p independent elements in $\mathcal{A}$. We are now ready to state the following.

Corollary 1. *Let $\mathcal{A}$ be the set identified by condition* I *for some input state, and suppose it contains q independent elements. Then the fraction of outputs in $G_{n,m}$ (i.e. including collision states) that condition* II *identifies as suppressed is equal to* $1 - \frac{1}{2^q} + O\left(\frac{\log m}{n}\right)$.

Proof. Suppose initially that there is a single element $A \in \mathcal{A}$, say $A = \{1\}$. The corresponding suppressed outputs are those whose BM representation contains an odd number of 1s in the first column. These consist of approximately half of all possible states, which can be seen as follows. Let us write the BM S of some such output as

$$S = \begin{pmatrix} \mathbf{S_1} & S' \end{pmatrix}, \tag{B.1}$$

where $\mathbf{S_1}$ is its first column and S' a matrix of the remaining $p - 1$ columns. Since all matrices that are equivalent up to a permutation of the rows correspond to the same state, we can assume without loss of generality that the 1s in $\mathbf{S_1}$ occupy the first slots. This means there are only $n + 1$ possibilities for $\mathbf{S_1}$, and it is easy to see that $n/2$ of them satisfy condition II. Since this holds irrespective of the choice of S', we conclude that $(n/2)/(n + 1) = 1/2 + O(1/n)$ out of all states are suppressed. The argument follows through almost unchanged for any A, even if it spans several columns. The above argument assumes that the number of states whose corresponding BM have k ones in the first column does not depend on k. While this is strictly true only in the approximation in which we count the number of states as if the particles are distinguishable, a more thorough calculation taking into account the bosonic statistics can be performed and leads to the same asymptotic result.

Suppose now $\mathcal{A}$ has q independent elements. By the previous paragraph, the first element of $\mathcal{A}$, let us call it A_1, leads to a suppression of approximately (i.e. up to $O(1/n)$) half of all outputs. The second element, A_2, also leads to a suppression of approximately half of all outputs—but now there is an overlap with those identified by A_1. Since the two are independent, approximately half of the elements identified by A_2 have already been identified by A_1 (e.g., approximately half of the matrices with an odd number of 1s in the first column also have an odd number of 1s in the second column). Thus the new suppressions identified by A_2 correspond only to $1/4 + O(1/n)$ of all states. Each subsequent independent element of $\mathcal{A}$ further divides the remaining set of unsuppressed states by half, and we conclude that condition II in fact identifies $1 - 1/2^q + O(q/n)$ of all states as suppressed. Since $q \leqslant p = \log(m)$, this gives the claimed asymptotic behavior. □

Corollary 1 shows that in the worst case, approximately $1/2$ of all outputs are suppressed for any input which satisfies condition I. This fraction can, in principle, be as high as $1 - 1/m$ if condition I identifies p independent elements in $\mathcal{A}$. It is thus essential to identify how many inputs effectively satisfy condition I in order to determine the overall fraction of suppressed pairs. Indeed, theorem 1 treats input and outputs asymmetrically, and as a consequence condition I is much more stringent than condition II.

Corollary 2. *Only an exponentially vanishing subset of the inputs is detected by the test of theorem* 1.

Proof. Let us begin by counting how many inputs have a particular element A in their set $\mathcal{A}$. Consider initially that $A = \{1\}$. For condition I to hold in this case, we need half of the elements of the first column of R to be 1 (see lemma 2). Since we are free to rearrange the rows as desired, we can assume that R is ordered as follows

$$R = \begin{pmatrix} \mathbf{1_{n/2}} & R_1 \\ \mathbf{0_{n/2}} & R_2 \end{pmatrix}, \tag{B.2}$$

where $\mathbf{1_{n/2}}$ and $\mathbf{0_{n/2}}$ are vectors of $n/2$ 1s and 0s respectively, and R_1 and R_2 are $(n/2) \times (p - 1)$ binary matrices. For R to satisfy $\mathcal{N}^{\{1\}}(R) \sim R$, we must have $R_1 \sim R_2$, and in fact we can further reorder the rows of R have such that $R_1 = R_2$. We can now count how many binary matrices satisfy these constraints. Clearly we have no choice over the first column and over R_2, so we only need count all possibilities for R_1. Given the form chosen for R above, it is clear that any two choices for R_1 that are equal upon permutation of the rows represent the same state, and should not be counted twice. This leads to a cumbersome combinatorial problem, since we need to tally all possibilities for R_1 up to permutations, but the number of permutations changes depending on whether R_1 has repeated rows. A shortcut to this calculation is to realize that we can formally map R_1 back to a MAL representation, as in section 2 and, subsequently to a quantum state of $n/2$ photons in $2^{p-1} = m/2$ modes. Thus, the number of possibilities for R_1 is $\binom{(n+m)/2-1}{n/2}$.

Consider next another possibility, that $A = \{1, 2\}$. The counting in this case is similar to before, but a little trickier, because we need to keep track of how many choices we have for the first two columns such that $\mathcal{N}^{\{1,2\}}(R) \sim R$. Let us once more order the matrix as follows

$$R = \begin{pmatrix} \mathbf{1_{n/2}} & \mathbf{a}_1 & R_1 \\ \mathbf{0_{n/2}} & \mathbf{a}_2 & R_2 \end{pmatrix}, \tag{B.3}$$

where $\mathbf{1_{n/2}}$ and $\mathbf{0_{n/2}}$ are defined as before, $\mathbf{a}_1$ and $\mathbf{a}_2$ are two binary vectors of length $n/2$ and R_1 and R_2 are $(n/2) \times (p-2)$ binary matrices. We want R to be ordered in such a way that $\mathcal{N}^{\{1,2\}}(R) \sim R$ implies $R_1 = R_2$, to reuse part of the previous argument. This immediately implies that $\mathbf{a}_2$ is obtained from $\mathbf{a}_1$ by negating its elements. We know that $\mathbf{a}_1$ and $\mathbf{a}_2$, together, must contain $n/2$ 1s, due to lemma 2, but that is already guaranteed by the fact that they are negations of each other[8]. From the freedom of reordering rows, we can assume that the 1s in $\mathbf{a}_1$ occupy the first positions. This leaves $(n/2 + 1)$ possibilities for $\mathbf{a}_1$. Combining that with the $\binom{(2n+m)/4-1}{n/2}$ possibilities for R_1 as in the previous paragraph, we get a total of $(n/2 + 1)\binom{(2n+m)/4-1}{n/2}$ possibilities. How does this compare with the case $A = \{1\}$? We can use the following asymptotic expression for the binomial coefficient $\binom{n}{k}$

$$\binom{n}{k} \approx \frac{(n-k/2)^k}{k^k e^{-k}\sqrt{2\pi k}}, \tag{B.4}$$

which holds when n is both large and much larger than k. By using this expression it is easy to see that, in the limit of both m and n large with $n \leqslant m$, $(n/2 + 1)\binom{(2n+m)/4-1}{n/2}$ grows exponentially slower than $\binom{(n+m)/2-1}{n/2}$, and so we can use the latter as an upper bound. In fact, as we consider sets A comprising of more columns, the constraints tend to become more restrictive and the number of matrices that satisfy them decreases. So we will use $\binom{(n+m)/2-1}{n/2}$ as an upper bound on the number of states that satisfy condition I for any A.

We are now ready to give an upper bound on the number of states that satisfy condition I for some non-empty $\mathcal{A}$. Since there are p columns in the binary matrices, There are $2^p - 1 = m - 1$ possible As that can appear in $\mathcal{A}$. By the inclusion-exclusion principle, we would need to sum the number of states that satisfy condition I for each possible A, then subtract those that have been counted multiple times because they satisfy it for more than one A. It is simpler, however, to use the union bound, which in this case says that the number of states is upper-bounded by $(m-1)\binom{(n+m)/2-1}{n/2}$. Recall now that the total number of states is $\binom{n+m-1}{n}$. Using an asymptotic formula for the binomial coefficient, it is clear that the fraction of states detected by the test is exponentially small in the limit of large n and m, as claimed.   □

In [40], the authors reach the same conclusion, using a different formalism, for the fraction of suppressed outputs given a specific input (i.e., corollary 1). However, they do not provide an estimate for the fraction of inputs that satisfy condition I (i.e., corollary 2).

So far, we have considered only the full set of states (i.e, including collision states) in the estimates of suppressed fractions, but the restriction to no-collision states is often more useful. For example, no-collision outputs are the only detected outcomes when the experiment is performed using bucket detectors (i.e. that do not distinguish one photon from many). More importantly, experimental implementations typically consider inputs with no more than a single photon per mode. This is also relevant for boson sampling applications, being input state with at most one photon per mode the appropriate choice for its computational hardness. Thus, it would be interesting to obtain versions of corollaries 1 and 2 where both the suppressed pairs and the set of all states included this restriction. Unfortunately, some pathological instances arise when we try to specialize the previous results in that way. To see that, consider the case where $n = m$. There, we have a single no-collision state, and it satisfies condition I. Thus, we conclude that 100% of inputs in that case have suppressed outputs. As we now argue, it is still possible to show a weaker version of corollary 2 for no-collision inputs.

Consider the regime where $m = \mathrm{O}(n^2)$. Experiments are often done in this limit, especially since it seems to be a requirement for the computational hardness of the boson sampling model [1]. It is easy to show that the set of no-collision states is not a negligibly subset of all states in this regime, due to the so-called birthday paradox. To illustrate this suppose $m = n^2$ holds exactly, in which case the fraction of no-collision states among all states is $\binom{n^2}{n} / \binom{n^2+n-1}{n}$. Using Stirling's approximation, one obtains that this tends to $1/e$ in the limit of large n. Since the set of no-collision states is only polynomially small in the set of all states, a no-collision version of corollary 2 must still hold—even if *all* inputs that satisfy condition I were concentrated in the no-collision subset, they would still be an exponentially small fraction of it. This argument shows that the conclusion of corollary 2 can be extended to the no-collision case in the limit $m = \mathrm{O}(n^2)$, and we leave it as an open question whether it holds in general.

Corollary 2 also has consequences for the application of theorem 1 as a test for validating boson sampling experiments. As argued in [24], suppressed events in Hadamard matrices (such as the Sylvester or Fourier

---

[8] Note that, whenever $\mathbf{a}_1$ has $1/4$ of the 1s, we are double-counting some matrices that were already included in the case $A = \{1\}$. But in the asymptotic limit they form a negligible fraction of the cases, so we do not worry about this correction.

matrices) could be useful as a way to witness partial photonic indistinguishability. Informally, the idea is that we only have suppressions of certain transitions if the particles are perfectly identical, and so observations of quantumly suppressed events could be used to estimate the degree of partial distinguishability of the photons. Corollary 2 shows that in Scattershot BosonSampling experiments [12, 25, 26], where inputs are chosen uniformly at random from all no-collision states, the number of suppressed events detected by theorem 1 vanishes exponentially. On the other side, when specific input states that satisfy condition I for many different As are employed, theorem 1 might provide a favorable scaling. Indeed, we showed that as many as $1 - O(1/m)$ out of all outcomes can be suppressed, but we leave a formal description of such a test for future work, as well as the question of whether the Sylvester matrix is optimal for this task.

Appendix C. Photon generation, manipulation and detection

Single photons were generated at 785 nm with a type-II PDC process in four PDC sources for scattershot configuration, pumping two crystals (2-mm long beta barium borate, BBO) with a 392.5 nm wavelength, 650 mW field, obtained by second harmonic generation from a 180 fs duration, 76 MHz repetition rate, Ti:Sa pulsed laser. Photons are spectrally filtered by means of 3 nm interferential filters and coupled into single-mode fibers. The indistinguishability of the photons is reached by means of a polarization compensation stage and by propagation through delay lines for each path before injection into the interferometer via a single-mode fiber array. After the evolution through the integrated devices, photons are collected via a multimode fiber array. The detection system for the scattershot experiment consists of four single-photon avalanche photodiodes for the 4-mode chip and other four for the heralding photons in the scattershot regime. Single-shot measurements have been performed with a 2-photon state produced by a single BBO crystal and injected in the 8-mode Sylvester interferometer. At the detection stage, eight avalanche photodiodes have been used to collect all output combinations. An 8-channel electronic data acquisition system (ID-800 by IDQuantique) allowed us to detect 2-photon coincidences between all output pairs and 4-photon coincidences (two injected plus two triggered) for all possible input states. LabView and C programs have been used to retrieve the coincidence events associated to all possible output combinations.

Appendix D. Model of the experiment

Here we discuss a theoretical model to describe the results of the experiment with the 4-mode device. In addition to the non-perfect unitary transformation (i), two sources of deviation from the ideal behavior contribute to the output measured pattern: (ii) multi-photon emission from the sources, and (iii) partial indistinguishability of the heralded photons.

As a preliminary step we characterized the parameters of the experimental setup. Typical singles count rates for the different sources are in the range 100–250 kHz, while two-fold coincidences are in the range 10–35 kHz. Such rates are measured by directly connecting the sources to single-photon detectors via single-mode fibers. By considering a detection efficiency of $\eta_{\mathrm{det}} \sim 0.55$ and the laser repetition rate of 76 MHz, we estimated the nonlinear gain g of the sources ($g \sim 0.12$ for C1, $g \sim 0.115$ for C2) and the coupling to single-mode fibers by finding numerically the values that best fit the measured rates. From this characterization, we also estimated the heralding probabilities to be η_i^T (in the range ~ 0.1–0.22 for the different sources). The overall transmissions from the delay lines to the output fiber-array are directly measured to be ~ 0.08–0.16, depending on the input–output combination. Thus, the overall transmission of the injected photon from the generation to the detection stage is estimated to be ~ 0.01–0.02 (including detection efficiency).

Multi-photon emission
Multi-photon emission arises due to the probabilistic nature of PDC. Indeed, there is a non-zero probability that two pairs are emitted from the same source within the same pulse. Ignoring terms with the emission of three or more pairs, the output state of each source can be approximated as

$$|\psi\rangle \sim |0, 0\rangle + g|1, 1\rangle + g^2|2, 2\rangle, \tag{D.1}$$

where g is the nonlinear gain of the source. Note that in our experiment, each PDC crystal corresponds to two different photon-pair sources as shown in figure 2 of the main text.

Let us consider the situation where an event is recorded by the heralding detectors corresponding to inputs (i, j), in coincidence with an event registered by the detectors placed at output modes (m, n). This event is assigned to the transition from the input combination (i, j) to the output one (m, n). The correct evolution is obtained when the sources on modes (i, j) generate a photon pair, the corresponding heralding detectors click, and two photons are detected on output modes (m, n). Multi-photon emission and non-photon number

resolving detectors result in additional patterns that can excite the same set of detectors. These patterns act as noise contributions that cannot be discriminated from the correct evolution. Two different contributions have to be considered. (a) Three different sources connected to input ports (i, j, k) emit a photon pair, while only the heralding detectors on modes (i, j) click. Hence, three-photons are effectively produced. If only the detectors on output modes (m, n) click (due to losses or the presence of more than one photon in the one output mode), this process cannot be discriminated from the correct evolution $(i, j) \rightarrow (m, n)$. (b) Only the sources connected to input ports (i, j) generate photons, but one of the two sources produces a double-pair event. This event cannot be discriminated in the heralding process with non-photon number resolving detectors. In this case, two-photons may be injected in the same input mode. Similarly to case (a), when only detectors on mode (m, n) click, this process cannot be discriminated from the correct evolution $(i, j) \rightarrow (m, n)$.

Partial photon indistinguishability

Partial distinguishability between the generated heralded photon arises due to spectral correlations between photons belonging to the same pair. Indeed, the two-photon term of a PDC source takes the following form

$$|\psi^{(2)}\rangle = \int d\omega_1 \int d\omega_2 f(\omega_1, \omega_2) a_1^\dagger(\omega_1) a_2^\dagger(\omega_2)|0, 0\rangle, \tag{D.2}$$

where $f(\omega_1, \omega_2)$ is the two-photon spectral amplitude. In general, spectral correlations are encoded in the function $f(\omega_1, \omega_2)$. When PDC sources are adopted as heralded single-photon sources, one of the two photons is detected to certify the presence of the twin photon. Due to the correlations encoded in the two-photon wave packet, the heralded photon will be in general in a mixed spectral state. This will result in a degree of partial distinguishability between the photons emitted by two identical sources. The effective joint density matrix describing the state of two heralded photons can be then approximated as

$$\rho^{(2)} = p|1, 1\rangle\langle 1, 1| + (1 - p)|1', 1''\rangle\langle 1', 1''|, \tag{D.3}$$

where $|1, 1\rangle$ stands for two indistinguishable photon, and $|1', 1''\rangle$ stands for two distinguishable particles. Here, p is an effective parameter describing the indistinguishability of the two photons. The parameter p can be characterized from the visibility of an HOM interference experiment performed with a 50:50 symmetric beamsplitter. In our case, the measured visibility between photons emitted from the two sources was $V^{(2)} = 0.724 \pm 0.008$. The parameter p can be retrieved from the value of $V^{(2)}$ by taking into account multiphoton emission, leading to $p = 0.758 \pm 0.008$.

ORCID iDs

Luca Innocenti ⓘ https://orcid.org/0000-0002-7678-1128

References

[1] Aaronson S and Arkhipov A 2011 The computational complexity of linear optics *Proc. 43rd Annual ACM Symp. on Theory of Computing* ed A Press pp 333–42
[2] Valiant L G 1979 The complexity of computing the permanent *Theor. Comput. Sci.* **8** 189–201
[3] Troyansky L and Tishby N 1996 Permanent uncertainty: on the quantum evaluation of the determinant and the permanent of a matrix *Proc. 4th Workshop on Physics and Computation (PhysComp'96)* (Boston, MA: Boston University)
[4] Broome M A, Fedrizzi A, Rahimi-Keshari S, Dove J, Aaronson S, Ralph T and White A G 2013 Photonic boson sampling in a tunable circuit *Science* **339** 794–8
[5] Spring J B *et al* 2013 Boson sampling on a photonic chip *Science* **339** 798–801
[6] Tillmann M, Dakic B, Heilmann R, Nolte S, Szameit A and Walther P 2013 Experimental boson sampling *Nat. Photon.* **7** 540–4
[7] Crespi A, Osellame R, Ramponi R, Brod D J, Galvão E F, Spagnolo N, Vitelli C, Maiorino E, Mataloni P and Sciarrino F 2013 Integrated multimode interferometers with arbitrary designs for photonic boson sampling *Nat. Photon.* **7** 545–9
[8] Spagnolo N *et al* 2013 General rules for bosonic bunching in multimode interferometers *Phys. Rev. Lett.* **111** 130503
[9] Spagnolo N *et al* 2014 Experimental validation of photonic boson sampling *Nat. Photon.* **8** 615–20
[10] Carolan J *et al* 2014 On the experimental verification of quantum complexity in linear optics *Nat. Photon.* **8** 621–6
[11] Carolan J *et al* 2015 Universal linear optics *Science* **349** 711–6
[12] Bentivegna M *et al* 2015 Experimental scattershot boson sampling *Sci. Adv.* **1** e1400255
[13] Loredo J C, Broome M A, Hilaire P, Gazzano O, Sagnes I, Lemaitre A, Almeida M P, Senellart P and White A G 2017 Boson sampling with single-photon fock states from a bright solid-state source *Phys. Rev. Lett.* **118** 130503
[14] Wang H *et al* 2017 High-efficiency multiphoton boson sampling *Nat. Photon.* **11** 361–5
[15] He Y *et al* 2017 Time-bin-encoded boson sampling with a single-photon device *Phys. Rev. Lett.* **118** 190501
[16] Seshadreesan K P, Olson J P, Motes K R, Rohde P P and Dowling J P 2015 Boson sampling with displaced single-photon Fock states versus single-photon-added coherent states: the quantum-classical divide and computational-complexity transitions in linear optics *Phys. Rev.* A **91** 022334
[17] Rohde P P, Motes K R, Knott P, Fitzsimons J, Munro W and Dowling J P 2015 Evidence for the conjecture that sampling generalized cat states with linear optics is hard *Phys. Rev.* A **91** 012342
[18] Tichy M C 2015 Sampling of partially distinguishable bosons and the relation to the multidimensional permanent *Phys. Rev.* A **91** 022316

[19] Tillmann M, Tan S-H, Stoeckl S E, Sanders B C, de Guise H, Heilmann R, Szameit A and Walther P 2015 Generalized multiphoton quantum interference *Phys. Rev. X* **5** 041015

[20] Shchesnovich V S 2015 Tight bound on the trace distance between a realistic device with partially indistinguishable bosons and the ideal bosonsampling *Phys. Rev. A* **91** 063842

[21] Renema J J, Menssen A, Clements W R, Triginer G, Kolthammer W S and Walmsley I A 2017 Efficient algorithm for boson sampling with partially distinguishable photons arXiv:1707.02793

[22] Aaronson S and Brod D J 2016 Bosonsampling with lost photons *Phys. Rev. A* **93** 012335

[23] Rahimi-Keshari S, Ralph T C and Caves C 2016 Sufficient conditions for efficient classical simulation of quantum optics *Phys. Rev. X* **6** 021039

[24] Tichy M C, Mayer K, Buchleitner A and Molmer K 2014 Stringent and efficient assessment of boson-sampling devices *Phys. Rev. Lett.* **113** 020502

[25] Scott Aaronson's blog, acknowledged to S Kolthammer (http://scottaaronson.com/blog/?p=1579)

[26] Lund A P, Laing A, Rahimi-Keshari S, Rudolph T, O'Brien J L and Ralph T C 2014 Boson sampling with a gaussian state *Phys. Rev. Lett.* **113** 100502

[27] Hamilton C S, Kruse R, Sansoni L, Barkhofen S, Silberhorn C and Jex I 2017 Gaussian boson sampling *Phys. Rev. Lett.* **119** 170501

[28] Aaronson S and Arkhipov A 2014 Bosonsampling is far from uniform *Quantum Inf. Comput.* **14** 1383–423

[29] Bentivegna M *et al* 2014 Bayesian approach to boson sampling validation *Int. J. Quantum Inf.* **12** 1560028

[30] Aolita L, Gogolin C, Kliesch M and Eisert J 2015 Reliable quantum certification of photonic state preparations *Nat. Commun.* **6** 8948

[31] Walschaers M, Kuipers J, Urbina J D, Mayer K, Tichy M C, Richter K and Buchleitner A 2016 Statistical benchmark for bosonsampling *New J. Phys.* **18** 032001

[32] Bentivegna M, Spagnolo N and Sciarrino F 2016 Is my boson sampler working? *New J. Phys.* **18** 041001

[33] Wang S T and Duan L M 2016 Certification of boson sampling devices with coarse-grained measurements arXiv:1601.02627

[34] Shchesnovich V S 2016 Universality of generalized bunching and efficient assessment of boson sampling *Phys. Rev. Lett.* **116** 123601

[35] Hong C K, Ou Z Y and Mandel L 1987 Measurement of subpicosecond time intervals between two photons by interference *Phys. Rev. Lett.* **59** 2044–6

[36] Tichy M C, Tiersch M, Melo F D, Mintert F and Buchleitner A 2010 Zero-transmission law for multiport beam splitters *Phys. Rev. Lett.* **104** 220405

[37] Crespi A, Osellame R, Ramponi R, Bentivegna M, Flamini F, Spagnolo N, Viggianiello N, Innocenti L, Mataloni P and Sciarrino F 2016 Suppression law of quantum states in a 3D photonic fast Fourier transform chip *Nat. Commun.* **7** 10469

[38] Su Z-E, Li Y, Rohde P P, Huang H-L, Wang X-L, Li L, Liu N-L, Dowling J P, Lu C-Y and Pan J-W 2017 Multiphoton interference in quantum fourier transform circuits and applications to quantum metrology *Phys. Rev. Lett.* **119** 080502

[39] Crespi A 2015 Suppression laws for multiparticle interference in Sylvester interferometers *Phys. Rev. A* **91** 013811

[40] Dittel C, Keil R and Weihs G 2017 Many-body quantum interference on hypercubes *Quantum Sci. Technol.* **2** 015003

[41] Osellame R, Taccheo S, Marangoni M, Ramponi R, Laporta P, Polli D, De Silvestri S and Cerullo G 2003 Femtosecond writing of active optical waveguides with astigmatically shaped beams *J. Opt. Soc. Am. B* **20** 1559–67

[42] Gattass R R and Mazur E 2008 Femtosecond laser micromachining in transparent materials *Nat. Photon.* **2** 219–25

[43] Tichy M C, Tiersch M, Mintert F and Buchleitner A 2012 Many-particle interference beyond many-boson and many-fermion statistics *New J. Phys.* **14** 093015

[44] Wanless I M 2005 Permanents of matrices of signed ones *Linear Multilinear Algebr.* **53** 427–33

[45] Tillmann M, Schmidt C and Walther P 2016 On unitary reconstruction of linear optical networks *J. Opt.* **18** 114002

[46] Hadzibabic Z, Stock S, Battelier B, Bretin V and Dalibard J 2004 Interference of an array of independent Bose–Einstein condensates *Phys. Rev. Lett.* **93** 180403

[47] Cennini G, Geckler R, Ritt G and Weitz M 2005 Interference of a variable number of coherent atomic sources *Phys. Rev. A* **72** 051601